

Mg-induced terahertz transparency of indium nitride films

H. Ahn, J.-W. Chia, H.-M. Lee, Y.-L. Hong, and S. Gwo

Citation: *Applied Physics Letters* **99**, 232117 (2011); doi: 10.1063/1.3669538

View online: <http://dx.doi.org/10.1063/1.3669538>

View Table of Contents: <http://scitation.aip.org/content/aip/journal/apl/99/23?ver=pdfcov>

Published by the [AIP Publishing](#)

Articles you may be interested in

Temperature dependence of terahertz optical characteristics and carrier transport dynamics in p-type transparent conductive CuCr_{1-x}Mg_xO₂ semiconductor films

Appl. Phys. Lett. **104**, 012103 (2014); 10.1063/1.4860994

Infrared to vacuum-ultraviolet ellipsometry and optical Hall-effect study of free-charge carrier parameters in Mg-doped InN

J. Appl. Phys. **113**, 013502 (2013); 10.1063/1.4772625

Mg doping of GaN grown by plasma-assisted molecular beam epitaxy under nitrogen-rich conditions

Appl. Phys. Lett. **96**, 132103 (2010); 10.1063/1.3374882

Terahertz emission mechanism of magnesium doped indium nitride

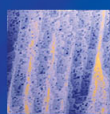
Appl. Phys. Lett. **95**, 232104 (2009); 10.1063/1.3270042

Terahertz emission from silicon and magnesium doped indium nitride

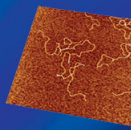
Appl. Phys. Lett. **93**, 221113 (2008); 10.1063/1.3043450

NEW! Asylum Research MFP-3D Infinity™ AFM

Unmatched Performance, Versatility and Support



Stunning high performance



Simpler than ever to GetStarted™

Comprehensive tools for nanomechanics



Widest range of accessories for materials science and bioscience



The Business of Science®



Mg-induced terahertz transparency of indium nitride films

H. Ahn,^{1,a)} J.-W. Chia,¹ H.-M. Lee,¹ Y.-L. Hong,² and S. Gwo²

¹Department of Photonics and Institute of Electro-Optical Engineering, National Chiao Tung University, Hsinchu 30010, Taiwan, Republic of China

²Department of Physics, National Tsing Hua University, Hsinchu 30013, Taiwan, Republic of China

(Received 11 September 2011; accepted 16 November 2011; published online 9 December 2011)

Terahertz time-domain spectroscopy (THz-TDS) has been used to investigate electrical properties of Mg-doped indium nitride (InN). Mg-doping in InN was found to significantly increase terahertz transmittance. THz-TDS analysis based on the Drude model shows that this high transmittance from Mg-doped InN is mainly due to the reduction in mobility associated with ionized dopants. The Hall-effect-measured mobility is typically lower than the THz-TDS-measured mobility for the same samples. However, the results of both measurements have the same slope in the linear relation between mobility and density. By introducing a compensation ratio of ~ 0.2 , an excellent agreement in mobilities of two methods is obtained. © 2011 American Institute of Physics. [doi:10.1063/1.3669538]

Recently, research activities in indium nitride (InN) have been dramatically increased due to its potential applications in high-frequency electronic devices and near-infrared optoelectronics. Due to its high electron affinity, as-grown InN is typically *n*-type and the growth and identification of *p*-type InN is one of the main challenges in the InN research. Recently, a series of works have been reported on the support of the presence of buried *p*-type conductivity in Mg-doped InN (InN:Mg),^{1–5} which is separated from the surface electron accumulation layer by a wide depletion layer. Typically, the electrical properties of InN:Mg are dominated by the surface layers and it is difficult to realize the true bulk conductivity of the buried bulk material. In fact, most of early works on InN have probed the material properties within the optical penetration depth (~ 133 nm for 800 nm optical pulse).⁶ In order to realize the true bulk material properties, it is necessary to perform a transmission measurement through a sufficiently thick sample and then the contribution from the surface region can be small when averaged over the whole film.

Here, we report the optical and electrical properties of InN:Mg as determined by terahertz time-domain spectroscopy (THz-TDS), which can measure the complex-valued electrical conductivity, carrier density, and mobility. Since THz transmittance through the film was measured in this experiment, the bulk conductivity and mobility could be unambiguously obtained. The results show that THz transmittance through the InN:Mg films is ~ 3 times larger than that measured for an undoped InN film. From the analysis of THz-TDS data with the Drude model, we found that the increase of THz transmission is associated with the reduction of the electrical conductivity and mobility, which is dominated by the electron scattering due to ionized dopants. The bulk mobility measured by THz-TDS shows a nearly carrier density-independent discrepancy with the mobility measured by the Hall effect. When the compensation of native donors with doped acceptors with a ratio of 0.2 is included in the

calculation, an excellent agreement is achieved in the mobilities measured by Hall effect and THz-TDS.

Wurtzite N-polar ($-c$ -axis), Mg-doped InN films with different carrier densities were grown by plasma-assisted molecular beam epitaxy on Si(111) substrates. The film thicknesses of samples are in the range of 1–1.5 μm . Mg doping was performed with a high-purity Mg (6N) Knudsen cell and the Mg doping level was controlled by regulating the cell temperature between 180 and 270 °C. An undoped InN film was also prepared as a reference material. The electron densities (N) and mobilities (μ) of samples are separately determined by room-temperature Hall effect measurements for comparison. The electron density determined by the Hall effect (N_{Hall}) is $2.0 \times 10^{18} \text{ cm}^{-3}$ for undoped InN film and N_{Hall} 's of InN:Mg films are in the range of 0.4 to $2.1 \times 10^{18} \text{ cm}^{-3}$. The THz-TDS system is based on a *p*-type InAs emitter excited and probed by a Ti:sapphire laser which delivers ~ 50 fs optical pulses at a center wavelength of 800 nm and a repetition rate of 1 kHz. Normally transmitted THz signal is detected by a free-space electro-optic sampling method. Since THz-TDS measures both the amplitude and the phase of the THz electric field, the absorption coefficient

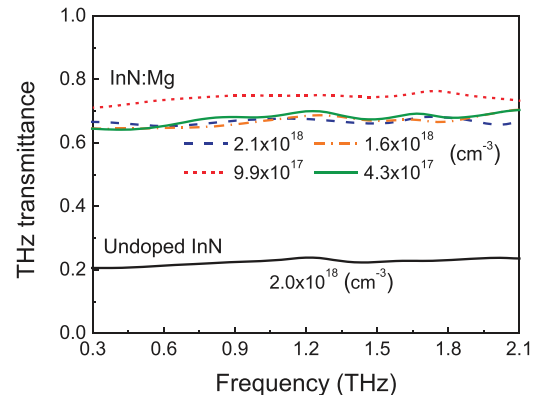
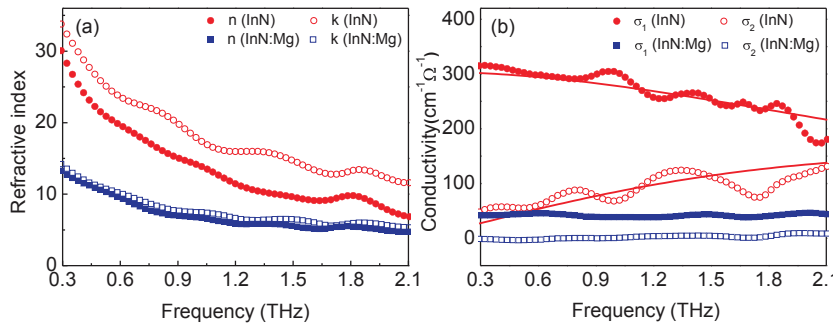


FIG. 1. (Color online) Terahertz transmittance of an undoped InN film and four Mg-doped InN films with different carrier densities. While that of the undoped film is about 0.2, terahertz transmittance of Mg-doped InN films is in the range of 0.65–0.7, nearly independent on the carrier density.

^{a)}Author to whom correspondence should be addressed. Electronic mail: hyahn@mail.nctu.edu.tw.



and refractive index can be extracted without the need of Kramers-Kronig analysis. The details of THz-TDS system can be found elsewhere.⁷

Figure 1 shows the transmittance of THz field in an undoped and four Mg-doped InN films (samples A, B, C, and D) with different carrier densities. The transmittance in each InN film was obtained by comparing the Fourier transformed THz electric field through the InN film to that through a Si(111) substrate. As shown in Fig. 1, the transmittances in InN:Mg films are much higher than that of the undoped InN film. Especially, sample A with a carrier density similar to the undoped InN film has THz transmittance at least three times higher than that of the undoped InN film. The complex refractive index (\tilde{n}) and the electrical conductivity ($\tilde{\sigma}(\omega) = \sigma_1 + i\sigma_2$) of the undoped InN film (circles) and sample A (squares) were obtained from frequency dependent THz transmittance in Fig. 1. As it can be seen in Fig. 2, monotonically decreasing \tilde{n} and the nearly frequency independent $\tilde{\sigma}$ of sample A are much smaller than those of the undoped InN film. We fit the measured complex conductivity in Fig. 2(b) using the simple Drude model, in which the complex conductivity is defined by

$$\tilde{\sigma}(\omega) = \epsilon_0 \omega_p^2 \tau_0 / (1 - i\omega\tau_0), \quad (1)$$

where ω_p is the plasma frequency and τ_0 is the carrier scattering time. For the undoped InN film, $\tilde{\sigma}(\omega)$ could be

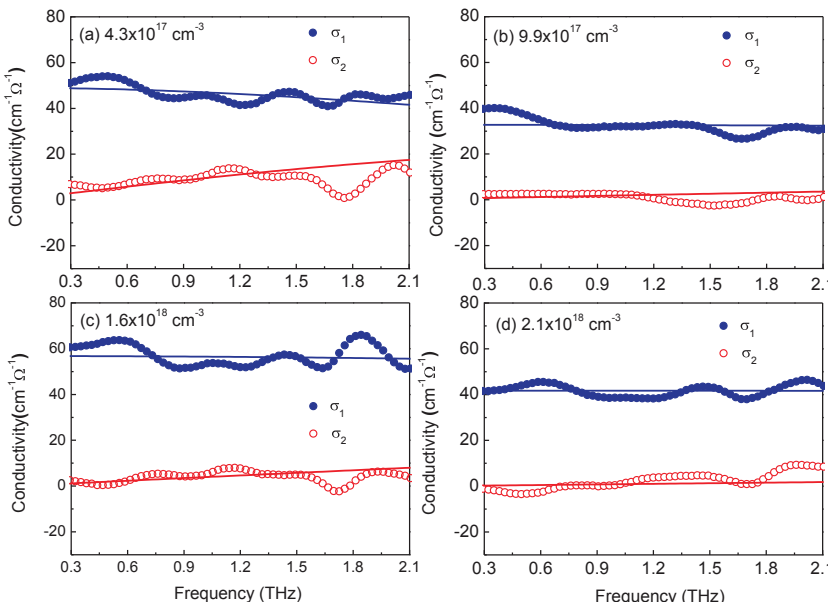


FIG. 2. (Color online) Complex refractive index (a) and conductivity (b) of the undoped- and Mg-doped InN (sample A) films. Refractive index and conductivity of sample A are much smaller than those of the undoped film.

replicated with the fitting parameters $\omega_p/2\pi = 39 \pm 1.2$ THz and $\tau_0 = 51 \pm 2.5$ fs. Assuming an electron effective mass $m_e^* = 0.075 m_0$ for InN,⁸ these fitting parameters correspond to an electron density $N_{\text{TDS}} = 1.4 \pm 0.2 \times 10^{18} \text{ cm}^{-3}$ and an electron mobility $\mu_{\text{TDS}} = 1195 \pm 50 \text{ cm}^2/\text{Vs}$. These values are in good agreement with Hall effect measurement results of $N_{\text{Hall}} = 2.0 \times 10^{18} \text{ cm}^{-3}$ and $\mu_{\text{Hall}} = 1120 \text{ cm}^2/\text{Vs}$, respectively.

Figure 3 depicts $\tilde{\sigma}(\omega)$ of InN:Mg samples obtained from the transmittance curves in Fig. 1. The complex conductivities of the InN:Mg films are again fitted with the Drude model in Eq. (1) and the fitting parameters are listed in Table I. It should be noted that the carrier scattering times of the InN:Mg films are much shorter than that of the undoped InN film whereas the plasma frequencies of the InN:Mg films are similar to that of the undoped film. The carrier lifetimes including cooling and diffusion time of the InN:Mg films have been studied separately.⁹ Especially, the spatial redistribution of carriers in diffusion and drift is found to be responsible for the recombination behavior as well as THz radiation.

The Drude model in Eq. (1) treats conduction electrons as free to move and subject to a collisional damping force. Therefore, the carrier scattering time obtained from our measurement corresponds to the average time between collisions. For doped semiconductors, free carriers are provided by the ionized dopants and among various carrier scattering mechanisms, scattering due to ionized centers is known to be

FIG. 3. (Color online) Frequency dependence of the complex conductivity of Mg-doped InN films grown at different Mg doping levels. The small conductivities of the Mg-doped InN films are mainly due to the reduction of the carrier scattering time as shown in Table I.

TABLE I. Extracted parameters for best fits in Figs. 2 and 3 compared to those obtained from Hall effect measurement.

Sample	ω_p (THz)	τ_0 (fs)	N_{TDS} (10^{18} cm^{-3})	μ_{TDS} (cm^2/Vs)	N_{Hall} (10^{18} cm^{-3})	$\mu_{Hall}(\mu_{TDS}^{0.2})$ (cm^2/Vs)
Undoped InN	39	51	1.4	1195	2.0	1120
A	36	9	1.2	204	2.1	137 (136)
B	39	11	1.4	255	1.6	176 (170)
C	28	12	0.71	287	0.99	192 (191)
D	21	34	0.40	747	0.43	530 (498)

most dominant for doped InN.¹⁰ For InN:Mg, the high density doping of Mg in InN increases the number of ionized centers and results in the reduction of collision time compared to that of the undoped InN film. Figure 4 summarizes the carrier density dependent mobility for InN:Mg samples, in which μ_{TDS} (black circles) is constantly larger than μ_{Hall} (red circles), whereas the slope in the linear relation between mobility and density measured for THz-TDS is in good agreement with the slope found for Hall effect measurements.

Because the contribution of surface layers to the bulk properties can be ignored for the thick samples ($\geq 1 \mu\text{m}$),¹¹ N_{TDS} and μ_{TDS} obtained by THz-TDS reflect the values in the bulk InN:Mg. In contrast, Hall effect measurement based on the van der Pauw method measures the material properties in two-dimensional, thin regions of samples and its result can be influenced by the existence of surface layers, including the surface accumulation layer and the depletion layer where the main carrier compensation occurs. In Kane's two-band model, the carrier scattering is affected by the non-parabolicity of the band and the electron mobility controlled by the scattering due to ionized centers can be expressed as¹²

$$\mu(k) = \frac{\varepsilon_0^2}{2\pi e^2 \hbar Z^2 N_i F_i} \left(\frac{dE}{dk} \right)^2 k, \quad (2)$$

where ε_0 is the static dielectric constant, Z is the charge of the ionized defects, and F_i is a k -dependent function. In an uncompensated material, the density of ionized defect centers N_i is given by $N_i = N_f/Z$, where N_f is the free electron density. In a compensated material, $N_i = N_f(1 + \theta)/(1 - \theta)$ is a function of the compensation ratio θ (ratio of minority to majority dopants).¹⁰ With a constant compensation ratio of

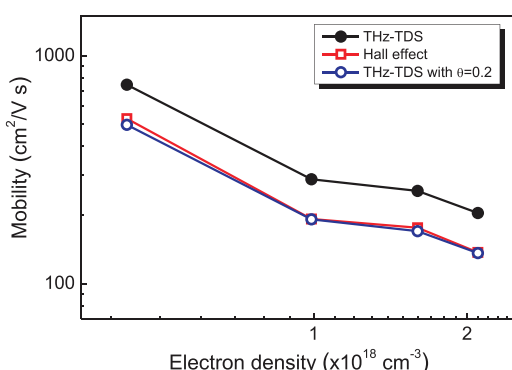


FIG. 4. (Color online) Electron-density-dependent electron mobility measured by the THz-TDS and the Hall-effect method. Open circles are THz-TDS-measured mobility corrected by including a compensation ratio $\theta = 0.2$.

$\theta = 0.2$, we obtained remarkably similar values of mobility $\mu_{TDS}^{0.2}$ (open circles in Fig. 4) to μ_{Hall} for InN:Mg. Meanwhile, according to the previous THz emission measurements from the same InN:Mg samples, the compensation ratio within the depletion layer varies with the carrier density.¹³ Therefore, the estimated value of $\theta = 0.2$ represents the averaged compensation ratio of the bulk InN:Mg comprising the carrier-density-dependent θ in the narrow depletion layer.

In summary, using the technique of THz spectroscopy, THz wave transmittance through Mg-doped InN was investigated. Since THz-TDS measurement is based on the transmittance through the samples, the measured material parameters correspond to the bulk properties of the samples. The refractive index and conductivity of InN:Mg were found to be much smaller than those of undoped InN and it is due to the reduction of carrier-carrier collision time. Electrical mobility of InN:Mg films show a linear relation with the carrier density, corresponding to electron scattering by ionized centers. The constant discrepancy of experimental results of THz-TDS and Hall effect measurement could be explained by the contribution of the carrier compensation between native donors and doped acceptors in the depletion layer.

This work was supported in part by the National Science Council (Grant No. NSC-99-2112-M-009-MY3) and a National Nanoscience and Nanotechnology Project (Grant No. NSC-99-2120-M-007-004).

- R. E. Jones, K. M. Yu, S. X. Li, W. Walukiewicz, J. W. Ager, E. E. Haller, H. Lu, and W. J. Schaff, *Phys. Rev. Lett.* **96**, 125505 (2006).
- X. Wang, S.-B. Che, Y. Ishitani, and A. Yoshikawa, *Appl. Phys. Lett.* **90**, 201913 (2007).
- P. D. C. King, T. D. Veal, P. H. Jefferson, and C. F. McConville, *Phys. Rev. B* **75**, 115312 (2007).
- Y. M. Chang, Y.-L. Hong, and S. Gwo, *Appl. Phys. Lett.* **93**, 131106 (2008).
- K. Wang, N. Miller, R. Iwamoto, T. Yamaguchi, M. A. Mayer, T. Araki, Y. Nanishi, K. M. Yu, E. E. Haller, W. Walukiewicz *et al.*, *Appl. Phys. Lett.* **98**, 042104 (2011).
- H. Ahn, C.-H. Shen, C.-L. Wu, and S. Gwo, *Appl. Phys. Lett.* **86**, 201905 (2005).
- H. Ahn, Y.-P. Ku, Y.-C. Wang, C.-H. Chuang, S. Gwo, and C. L. Pan, *Appl. Phys. Lett.* **91**, 163105 (2007).
- J. Wu, W. Walukiewicz, W. Shan, K. M. Yu, J. W. Ager III, E. E. Haller, H. Lu, and W. J. Schaff, *Phys. Rev. B* **66**, 201403 (2002).
- H. Ahn, K.-J. Yu, Y.-L. Hong, and S. Gwo, *Appl. Phys. Lett.* **97**, 062110 (2010).
- R. E. Jones, S. X. Li, L. Hsu, K. M. Yu, W. Walukiewicz, Z. Liliental-Weber, J. W. Ager III, E. E. Haller, H. Lu, and W. J. Schaff, *Physica B* **376-377**, 436 (2006).
- P. D. C. King, T. D. Veal, and C. F. McConville, *J. Phys.: Condens. Matter* **21**, 174201 (2009).
- W. Zawadzki and W. Szymanska, *Phys. Status Solidi B* **45**, 415 (1971).
- H. Ahn, Y.-J. Yeh, Y.-L. Hong, and S. Gwo, *Appl. Phys. Lett.* **95**, 232104 (2009).